IEEE Access
Multidisciplinary | Rapid Review | Open Access Journal

Received 6 February 2024, accepted 17 February 2024, date of publication 27 February 2024, date of current version 5 March 2024.

Digital Object Identifier 10.1109/ACCESS.2024.3371158

RESEARCH ARTICLE

Parallel Self-Tuning Controllers for Speed Servo System Based on Predictive Model-Mismatch Compensation

FENG DAN, HUILAN HE, SHAOWU LU, AND YAJIE MA
School of Information Science and Engineering, Wuhan University of Science and Technology, Wuhan 430081, China

Corresponding author: Shaowu Lu (shawn2013@wust.edu.cn)

This work was supported in part by the National Natural Science Foundation of China under Grant 51975430, and in part by Hubei Provincial Science and Technology Plan Project under Grant 2023DJC173 and Grant 2023DJC176.

ABSTRACT When the operating conditions are changed suddenly, the model mismatch for the servo system using model-based methods occurs during the identification convergence, which will lead to the obvious speed spikes and damped oscillations, deteriorating the control performance of the servo system. To solve the problem, a parallel self-tuning scheme based on a generalized predictive control law is proposed in this paper. In the proposed scheme, the controlled model parameters in which an integral-proportional controller (IPC) is considered as the controller of speed loop are first online estimated by a recursive least squares method with a forgetting factor. Then, a model-mismatch compensator (MMC) is designed to obtain the corresponding compensation current, and in addition, the predicted speed is considered as the feedback speed to promote the establishment of an inner loop, which allows for a faster and more thorough model mismatch compensation based on both the excitation torque current and the adaptivity of the MMC. At the same time, through constructing two different quadratic performance indicators, the optimal control laws can be obtained based on a simplified decoupled derivation, thus supplying IPC and MMC with suitable control parameters simultaneously. Simulation and experimental results show that, compared with traditional methods, the proposed scheme can ensure faster convergence speed and better control performance.

INDEX TERMS Servo system, generalized predictive control, model-mismatch compensator, integral proportional, self-tuning.

I. INTRODUCTION

With the rapid development of power electronics technology, high-frequency high-power switching devices and new control theory, permanent magnet synchronous motors (PMSMs) have been more and more widely used in many fields [1], [2], [3]. However, in the actual operation, the controlled object of the PMSM servo system is typically nonlinear because of the obvious external disturbances and system delay, and in addition, conventional linear controllers, e.g., proportional integral control (PIC) [4] and active disturbance rejection control (ADRC) [5], are utilized to adjust the tracking performance but cannot maintain the satisfactory control performance when the system is in the operation conditions of time-varying load inertia or load torque. Fortunately, scholars have developed some nonlinear control algorithms in recent years, such as sliding-model control (SMC) [6], [7], model predictive control (MPC) [8], [9], and adaptive backstepping control [10], [11], which can guarantee a superior control performance of the system. However, the structure of these nonlinear control algorithms is relatively more complex and sensitive to the choice of initial values, which is not favorable for engineers. In contrast, the integral-proportional controller (IPC) has been widely used for its simplicity, anti-interference and robustness [12], [13]. To further obtain the satisfactory set-point tracking performance, it is more

The associate editor coordinating the review of this manuscript and approving it for publication was Feifei Bu.

noteworthy that it is also extremely necessary for a self-tuning IPC to automatically adjust its control parameters according to complex operating conditions [14].

An increasing number of scholars, at the moment, provide control parameters using various intelligent or control algorithms, which can be roughly divided into two categories: Rule-based methods [14], [15], [16] and model-based methods. The rule-based methods, e.g., the particle swarm optimization algorithm [14], the fuzzy idea [15], the Neural Network algorithm [16], do not rely on accurate mathematical models, but the computational complexity is considerable. The model-based methods, however, are more feasible for the cases where online tuning is required, such as internal model principle (IMP) [17], just-in-time learning (JITL) [18], and generalized predictive control (GPC) [19], [20], [21], [22], [23], [24], [25], [26]. Among them, in comparison to the IMP and FITL, the GPC-based self-tuning method draws more and more attention due to its robustness and anti-interference capability. The main idea is to map the GPC control law obtained by the identification algorithm to a simple PIC or IPC by correcting the reference instruction and predictive model. Nevertheless, it is worth noting that in [19], [20], and [21], when the operating conditions of the PMSM servo system are changed suddenly, the model mismatch occurs in the identification convergence process, which will lead to the obvious speed spikes and damped oscillations, deteriorating the control performance. In [22] and [23], a disturbance observer was designed to accomplish the mismatch compensation caused by the load disturbance, but it could not work on the sudden inertia change.

Generally, there may be two different ways to solve the model-mismatch problem in theory. On the one hand, according to the principle of online identification, the high-prediction model can also be modified directly by some advanced identification algorithms. Koryakovskiy et al. [24] proposed a reinforcement learning algorithm to train and correct the controlled model. But the training cost and computational complexity are too expensive. On the other hand, the future error can be predicted and compensated on the basis of keeping the estimated model unchanged [25]. In [26], a SMC-based compensator was designed to provide model mismatch-induced loss currents in real-time, however, the sliding-mode chattering problem was not solved. In addition, the above mismatch compensators are fixed-parameter and missing adaptivity, which is apparently contrary to the original GPC-based self-tuning controller.

Through the above analysis, this paper proposes a parallel self-tuning scheme for servo speed control. First, the model parameters are identified by a recursive least squares method with a forgetting factor (FFRLS) to obtain a linearized estimation model. Then, a model-mismatch compensator (MMC) is designed to obtain the corresponding compensation current. Finally, based on two different quadratic performance indicators, the optimal control laws can be obtained by simplified decoupled derivation, and two controllers are simultaneously mapped by a GPC algorithm. In contrast to the previous work,

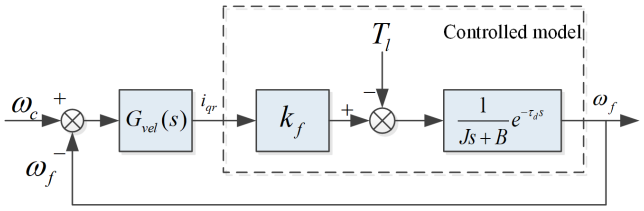

FIGURE 1. Speed loop schematic diagram of the PMSM servo system.

the main contributions in this paper are: 1) A GPC-based MMC, in which the adaptive characteristics allows it to flexibly address model mismatches caused by a variety of operating conditions, is designed to obtain the corresponding compensation current. 2) The predicted speed is considered as the feedback speed to promote the establishment of an inner loop, which allows for a faster and more thorough model mismatch compensation based on the excitation torque current and the adaptivity of the MMC, and makes the speed error between actual speed and predicted speed decay to zero. 3) Through reconstructing two different quadratic performance indicators, both the IPC and the MMC are simultaneously mapped by a GPC algorithm, which reduces the computational complexity.

II. MODELLING OF THE SERVO SYSTEM

A. SPEED LOOP MODELLING

On the basis of the PMSM vector control, the static three-phase AC can be converted to the rotating two-phase DC, making it possible to achieve high-performance current regulation. With the decoupling control of zero excitation current, the two-phase DC can be guaranteed the perfect current tracking respectively, and at the same time, the delay time for the speed control system is heavily distributed in the dead time of inverter [27]. As a consequence, the speed model dynamics of the PMSM servo system is revealed in Fig.1, and its Laplace domain can be processed as follows:

$$\omega_f(s) = \frac{k_f i_{qr}(s) - T_l}{Js + B} e^{-\tau_d s} \tag{1}$$

where ω_c and ω_f are the command speed and actual speed respectively; i_{qr} is the torque current, k_f is the torque coefficient, J is the rotor inertia; B is the friction factor, T_l is tehe load torque, τ_d is the system's dead time.

B. SIMPLIFIED MODEL

In the actual industrial applications of the servo system, many cheering research reports, in general, consider the linear model as controlled model for simplifying the algorithms complexity [28], [29]. To apply the predictive control into the speed control system, consequently, a first-order linear model can be required for reducing the online implementation burden [30]. And more notably, the application development of the GPC algorithm is further extended by utilizing a dynamic first-order linear model instead of the nonlinear control object. Therefore, equation (1) can be simplified and

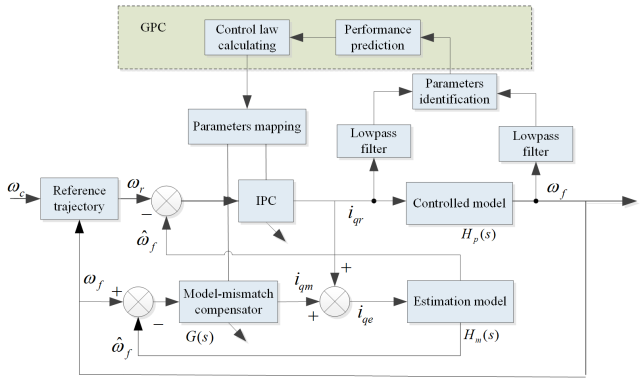

FIGURE 2. The overall schematic diagram.

described by the following discrete difference equations:

$$O(z^{-1})\omega_f(n) = P(z^{-1})i_{qr}(n-1) \tag{2}$$

$$O(z^{-1}) = 1 + a_1 z^{-1} \tag{3}$$

$$P(z^{-1}) = b_1 \tag{4}$$

where $a_1 = \frac{T_s \cdot B}{J} - 1$ and $b_1 = \frac{T_s \cdot k_f}{J}$ are the model parameters to be estimated; T_s and n is the sampling time and the time index, respectively.

In this paper, the IPC, as the speed loop controller, has advantages in robustness and immunity to interference compared to the PIC [20]. As a result, the incremental IPC structure can be described as:

$$\Delta i_{qr}(n) = k_{I1}[\omega_c(n) - \omega_f(n)] - k_{P1}\Delta\omega_f(n) \tag{5}$$

$$i_{qr}(n) = i_{qr}(n-1) + \Delta i_{qr}(n) \tag{6}$$

where k_{p1} is the proportional parameter, k_{I1} is the integral parameter, $\Delta = 1 - z^{-1}$ is the difference operator.

III. DESIGN OF PARALLEL SELF-TUNING CONTROLLERS

Here, since the derivation to the GPC requires an exact controlled model, it is first necessary to identify the model parameters in real-time by the FFRLS algorithm. When the PMSM runs under the complex operating conditions, the estimated model will not exactly match with the actual model due to the slow identification convergence. During the convergence process, the based-GPC IPC cannot match the operating conditions, and results in obvious speed peak and damped oscillations. In this paper, therefore, the predicted speed calculated online is taken as the feedback speed to promote the larger torque current, and the MMC is combined to compensate for the model mismatch. At the same time, both the IPC and MMC are mapped by a GPC law simultaneously. The overall parallel scheme is shown in Fig. 2.

A. PARAMETERS IDENTIFICATION

Through minimizing the estimated output error, the FFRLS method has capable of estimating online the linear system model with the sudden load inertia or load torque. It is important to note that the nonlinear term load torque can be fitted to the linear model by the FFRLS, thus equating to the variation of the model parameters, in order to improve the adaptivity of the controller against load disturbances. The detailed identification process is as follows:

$$\hat{\rho}(n) = \hat{\rho}(n-1) + K(n)[\omega_f(n) - \hat{\rho}(n-1)\zeta^T(n-1)] \tag{7}$$

$$K(n) = \frac{\psi(n-1)\zeta(n-1)}{\alpha^* + \zeta^T(n-1)\psi(n-1)\zeta(n-1)} \tag{8}$$

$$\psi(n) = \frac{1}{\alpha^*}[\psi(n-1) - \frac{\psi(n-1)\zeta^T(n-1)\psi(n-1)\zeta(n-1)}{\alpha^* + \zeta^T(n-1)\psi(n-1)\zeta(n-1)}] \tag{9}$$

$$\hat{\rho}(n) = [a_1(n), b_1(n)] \tag{10}$$

$$\zeta(n-1) = [-\omega_f(n-1), i_{qr}(n-1)] \tag{11}$$

where, α^* is forgetting factor, $\psi(0) = \delta I(0 < \delta < \infty)$.

B. MODEL-MISMATCH COMPENSATOR

However, as consistent with other identification algorithms, the convergence process of the parameters identified by the FFRLS algorithm is prone to model mismatch, resulting in obvious speed peak and damped oscillations. To reduce the model mismatch error, the predicted speed is used as the feedback speed so that the controlled estimated model fits better into the servo system. However, it will lead to the disconnection between the actual speed and the predicted speed. Therefore, in this paper an inner loop using the MMC is built as the model mismatch compensation, which can ensure the model-following error to decay asymptotically to zero with fast dynamic response with respect to the outer speed loop. The equation is established as follows:

$$\Delta i_{qm} = k_{I2}[\omega_f(n) - \hat{\omega}_f(n)] - k_{P2}\Delta\hat{\omega}_f(n) \tag{12}$$

$$i_{qm}(n) = i_{qm}(n-1) + \Delta i_{qm}(n) \tag{13}$$

$$\hat{\omega}_f(n) = -a_1(n)\hat{\omega}_f(n-1) + b_1(n)i_{qe}(n-1) \tag{14}$$

where, k_{P2} is the proportional parameter, k_{I2} is the integral parameter, $\hat{\omega}_f(n)$ is the predicted speed.

Since the predicted speed is considered as the feedback speed, and the speed command is smoothed to obtain the reference trajectory ω_r, (5) can be rewritten as following (15), and in addition, the corresponding compensation current based on the MMC can speed up the dynamic response and significantly reduce the speed spikes when sudden changes occur. So the total current torque can be expressed as (16).

$$\Delta i_{qr}(n) = k_{I1}[\omega_r(n) - \hat{\omega}_f(n)] - k_{P1}\Delta\hat{\omega}_f(n) \tag{15}$$

$$i_{qe}(n) = i_{qr}(n) + i_{qm}(n) \tag{16}$$

C. PERFORMANCE PREDICTION

Here, two different quadratic performance indicators need to be defined to obtain two sets of control parameters, and so the secondary performance indicators of the IPC and MMC are

as follows:

$$\begin{cases} J_{IP} = \sum_{j=N_1}^{N_2} [\hat{\omega}_f(n+j) - \omega_r(n+j)]^2 \\ \qquad +\lambda \sum_{j=1}^{N_u} \Delta i_{qr}(n+j-1)^2 \\ J_{MMC} = \sum_{j=N_1}^{N_2} [\hat{\omega}_f(n+j) - \omega_f(n+j)]^2 \\ \qquad +\lambda \sum_{j=1}^{N_u} \Delta i_{qm}(n+j-1)^2 \end{cases} \tag{17}$$

where $\hat{\omega}_f(n+j)$ is the predicted speed after j steps, N_1, N_2, N_u, and λ are the minimum prediction range, maximum prediction range, control range, and control increment weighting factors, respectively. Note that in general, $N_1 = 1$, $N_u \leq N_2$.

To obtain the predicted speed after j steps, the simplified Diophantine equations are processed as:

$$1 = S_j(z^{-1})O(z^{-1})\Delta + z^{-j}T_j(z^{-1}) \tag{18}$$
$$S_j(z^{-1})P(z^{-1}) = U_j(z^{-1}) \tag{19}$$
$$S_j(z^{-1}) = s_0 + s_1 z^{-1} + \ldots + s_j z^{-j+1} \tag{20}$$
$$T_j(z^{-1}) = t_0^j + t_1^j z^{-1} \tag{21}$$
$$U_j(z^{-1}) = b_1(s_0 + s_1 z^{-1} + \ldots + s_j z^{-j+1}) \tag{22}$$

Based on the simplified Diophantine equations, the speed output at the optimal prediction moment is given by:

$$\hat{\omega}_f(n+j) = U_j[\Delta i_{qm}(n+j-1) + \Delta i_{qr}(n+j-1)] + T_j\hat{\omega}_f(n) \tag{23}$$

Equation (23) is rewritten in vector form and it is given by:

$$\vec{\omega} = U(\vec{i}_{qm} + \vec{i}_{qr}) + \vec{T}\hat{\omega}_f(n) \tag{24}$$

where,

$$\vec{\omega} = [\hat{\omega}_f(n+N_1), \ldots, \hat{\omega}_f(n+N_2)]^T \tag{25}$$
$$\vec{i}_{qr} = [\Delta i_{qr}(n), \ldots, \Delta i_{qr}(n+N_u-1)]^T \tag{26}$$
$$\vec{i}_{qm} = [\Delta i_{qm}(n), \ldots, \Delta i_{qm}(n+N_u-1)]^T \tag{27}$$
$$\vec{T} = [T_{N_1}(z^{-1}), \ldots, T_{N_2}(z^{-1})]^T \tag{28}$$
$$U = \begin{bmatrix} b_1 s_0 & & & \\ b_1 s_1 & b_1 s_0 & & \\ \cdot & & & \\ b_1 s_{N_u-1} & b_1 s_{N_u-2} & \cdot & b_1 s_0 \\ \cdot & & & \\ b_1 s_{N_2-1} & b_1 s_{N_2-2} & \cdot & b_1 s_{N_2-N_u} \end{bmatrix} \tag{29}$$

According to the above definition, the quadratic performance index functions can be written as:

$$\begin{cases} J_{IPC} = [\vec{\omega} - \vec{\omega}_r]^T[\vec{\omega} - \vec{\omega}_r] + \lambda \vec{i}_{qr}^T \vec{i}_{qr} \\ J_{MMC} = [\vec{\omega} - \vec{\omega}_f]^T[\vec{\omega} - \vec{\omega}_f] + \lambda \vec{i}_{qm}^T \vec{i}_{qm} \end{cases} \tag{30}$$

where,

$$\vec{\omega}_r = [\omega_r(n+N_1), \ldots, \omega_r(n+N_2)]^T \tag{31}$$
$$\vec{\omega}_f = [\omega_f(n+N_1), \ldots, \omega_f(n+N_2)]^T \tag{32}$$

In order to obtain the optimal solutions of $\vec{i}_{qr}$ and $\vec{i}_{qm}$, the partial derivative of (30) can be processed as:

$$\begin{cases} U^T[U(\vec{i}_{qr} + \vec{i}_{qm}) + \vec{T}\hat{\omega}_f(n) - \vec{\omega}_r] + \lambda \vec{i}_{qr} = 0 \\ U^T[U(\vec{i}_{qr} + \vec{i}_{qm}) + \vec{T}\hat{\omega}_f(n) - \vec{\omega}_f] + \lambda \vec{i}_{qm} = 0 \end{cases} \tag{33}$$

It is noted that $\vec{i}_{qr}$ and $\vec{i}_{qm}$ from (30) are coupled, but if $\vec{i}_{qr}$ and $\vec{i}_{qm}$ act as the disturbances to the corresponding closed loop, the decoupled solutions can be obtained as:

$$\begin{cases} \vec{i}_{qr} = (U^T U + \lambda I)^{-1} U^T[\vec{\omega}_r - \vec{T}\hat{\omega}_f(n)] \\ \vec{i}_{qm} = (U^T U + \lambda I)^{-1} U^T[\vec{\omega}_f - \vec{T}\hat{\omega}_f(n)] \end{cases} \tag{34}$$

According to the principle and characteristics of GPC, the control laws can be derived as:

$$\begin{cases} \Delta i_{qr}(n) = V(z^{-1})\omega_r(n+N_1) - T(z^{-1})\hat{\omega}_f(n) \\ \Delta i_{qm}(n) = V(z^{-1})\omega_f(n+N_1) - T(z^{-1})\hat{\omega}_f(n) \end{cases} \tag{35}$$

where,

$$V(z^{-1}) = v_{N_2} + v_{N_2-1} z^{-1} + \ldots + v_{N_1} z^{-(N_2-N_1)} \tag{36}$$
$$[v_{N_1} \ldots v_{N_2}] = [1\ 0 \ldots 0](U^T U + \lambda I)^{-1} U^T \tag{37}$$
$$\begin{aligned} T(z^{-1}) &= v_{N_1} T_{N_1}(z^{-1}) + v_{N_1+1} T_{N_1+1}(z^{-1}) \\ &\quad + \ldots + v_{N_2} T_{N_2}(z^{-1}) \\ &= t_0 + t_1 z^{-1} \end{aligned} \tag{38}$$

D. PARAMETERS MAPPING

Since the required speed command is typically a step signal, the set point between the current command and the future command is identical [20]. As a consequence, equation (35) can be rewritten as:

$$\begin{cases} \Delta i_{qr}(n) = v_r\omega_r(n) - (t_0 + t_1 - t_1\Delta)\hat{\omega}_f(n) \\ \Delta i_{qm}(n) = v_r\omega_f(n) - (t_0 + t_1 - t_1\Delta)\hat{\omega}_f(n) \end{cases} \tag{39}$$

$$v_r = \sum_{j=N_1}^{N_2} v_j \tag{40}$$

Based on $t_0^j + t_1^j = 1$, comparing (12) and (15) with (39), the control parameters of both IPC and MMC are processed as:

$$\begin{cases} k_{I1} = (t_0 + t_1), k_{P1} = -t_1 \\ k_{I2} = (t_0 + t_1), k_{P2} = -t_1 \end{cases} \tag{41}$$

E. REFERENCE TRAJECTORY

To reduce the overshoot caused by command mutation, an idea base on the reference trajectory is utilized to make the predicted speed transition smoothly to the speed command.

The reference trajectory is taken as the following first-order smoothing model.

$$\begin{cases} \omega_r(n+j) = \varepsilon\omega_r(n+j-1) + (1-\varepsilon)\omega_c(n), \\ \qquad\qquad j = 1, 2, \ldots, N \\ \omega_r(n) = \omega_f(n) \end{cases} \tag{42}$$

where, $\varepsilon \in [0, 1)$.

Remark 1: It is noted that the dynamic performance of the GPC law is affected by the value of N_2. When the value of N_2 is small, the servo system will have a poor dynamic response. When the value of N_2 increases, the dynamic performance will be improved significantly. However, N_2 cannot be too large, which will obviously increase the computational burden.

Remark 2: The stability of the GPC law has been demonstrated in [28]. In the proposed scheme, the control laws of both closed loops are given by the GPC law. Therefore, The error $e(n) = \omega_c(n) - \omega_f(n)$ will eventually converge to 0.

Remark 3: It can be noticed from (2)-(4) that the load torque term is ignored during the design process, which is allowed benefiting from the better disturbance immunity of the IPC itself [19], [20], [21]. Besides, when the load torque occur, the FFRLS is able to fit the nonlinear disturbances to the estimated model parameters, which can be equivalent to the change of the model parameters, so as to promote the adaptability of controller parameters, and finally further improve the anti-interference ability of the controller.

IV. SIMULATION

Here, the proposed control method will be simulated using MATLAB/Simulink in conjunction with simulation conditions shown in Table 1. The parameters of the PMSM servo system are given by Table 2, the saturation limits of i_{qr}, i_{qm} and i_{qe} are all 15A, and the control period T_s of the speed loop is 5ms, respectively. The related parameters of GPC and FFRLS are set the same as those set in [20], i.e., $N_1 = 1$, $N_2 = 10$, $N_u = 2$, $\lambda = 0.01$, $\alpha^* = 0.9$, $\varepsilon = 0.2$ and $\delta = 10^3$.

The detailed processes of proposed scheme are shown in Fig. 3. To comprehensively verify the validity of the proposed scheme, five different methods, which include the PI controller, the ADRC method in [5] ($k_{ps} = 1.36$), the MPC with ESO method in [8] ($p = 20$), the GPC-based IPC, and the proposed method, are considered for the performance comparison at Cases 1-3. Among them, the relating initial parameters are set to $a_1(0) = 0.1$, $b_1(0) = 0.1$, $k_{P1}(0) = 0.25$, and $k_{I1}(0) = 0.12$.

The simulation results of the five controllers at Cases 1-3 are demonstrated in Figs. 4-9. At Case 1, i.e., when there is a sudden change in the motor inertia, the speed responses in Fig. 4(a) shows that the PIC and the MPC with ESO have different degrees of undamped oscillations, which is due to the fact that the fixed control parameters are not able to flexibly deal with the sudden change in operating conditions, and meanwhile, the ADRC controller inevitably generates damped oscillation due to the uncertainty of model parameters. On the contrary, the other two GPC-based controllers have the ability to avoid this situation to a large extent due to the adaptive nature of the control parameters caused by the change of model parameters as shown in Fig. 5. However, it should be noted that because of the effect of model mismatch, the GPC-based IPC illustrates more significant fluctuations compared to our method. This phenomenon can be clearly verified from the torque currents in Fig. 4(b). At Case 2, i.e., When $0.3 \leq t < 0.5s$, the load torque is increased to the PMSM, the speed response based on the PIC collapses rapidly, and there is a significant speed static difference. However, the ADRC method, the MPC with ESO method, the GPC-based IPC and the proposed method are all capable of eliminating the speed error and have excellent anti-disturbance ability, but the difference between these three controllers is that the proposed method can promote faster speed convergence, and has smaller speed peaks at the instant of adding the load toque, which is also verified by the torque currents in Fig. 6(b). The control parameters and model parameters of the proposed scheme are demonstrated in Fig. 7. Additionally, when $t = 0.2s$, in Figs. 4(a) and 6(a), the command is abruptly changed, the PIC, the ADRC, the MPC with ESO, and the GPC-based IPC have different degrees of overshoot. The comparison indicates that the proposed scheme can effectively reduce the overshoot after smoothing the speed command.

To further verify the anti-interference capability of the proposed method, as in Figs. 8 and 9, we simulated Case 3, i.e., adding the load torque with sinusoidal variations to the PMSM. It is easy to see that the PIC still exhibits poor anti-interference ability, followed by the GPC-based IPC, which has a more significant improvement due to the advantage of the GPC-based adaptive controller itself. It is noted that, however, as a consequence of the persistence of the model mismatch, large error peaks and speed fluctuations still exist compared to the ADRC method, the MPC with ESO method, and our method. This is made possible by the fact that our MMC is capable of providing compensation currents of the model mismatch in real time. Table 3 presents a quantitative comparison of these five controllers involving root mean square error (RMSE), settling time (ST), and maximum oscillation amplitude (MOA). This comprehensively validates the competitiveness of the proposed method in terms of control performance, robustness, and immunity to interference.

V. EXPERIMENT

This experimental study will be carried out on the platform in Fig. 10. The experimental setup mainly includes five parts: 1) A PMSM whose parameters are shown in Table 2. 2) A servo driver uses TI TMS320F28069 DSP chip as the main processor to complete the analysis of the digital incremental encoder, and its main function is to realize the speed control of PMSM. 3) A controller using TI TMS320F28335 DSP chip to carry out data transmission through CAN bus. 4) A host is used to debug, send speed commands and parameters to the controller, and receive

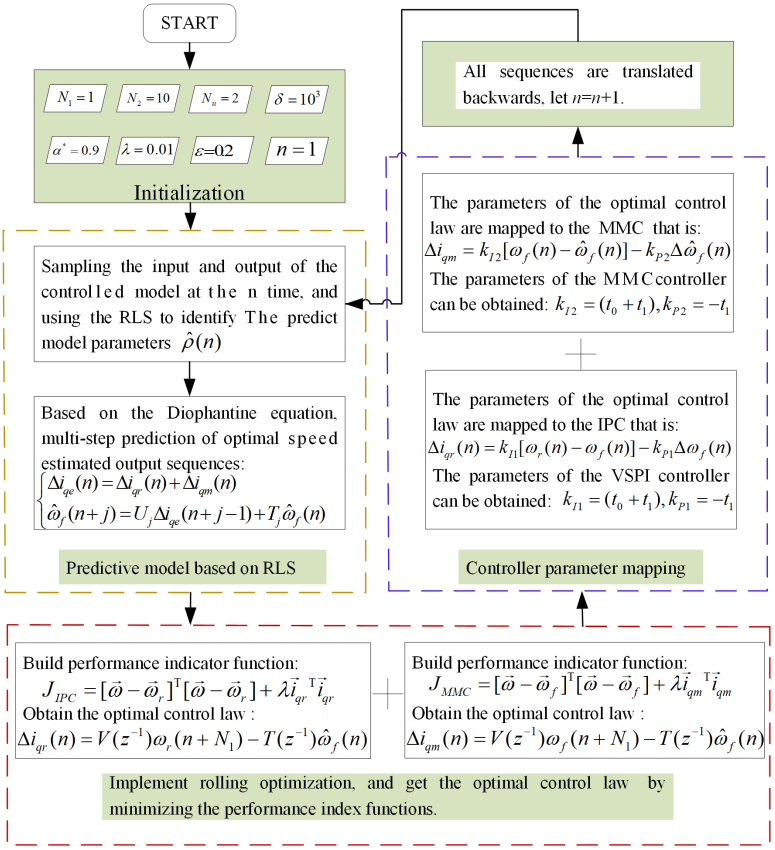

FIGURE 3. Design flow chart of proposed scheme.

TABLE 1. Simulation conditions.

Condition	Simulation content			
case1	Refe. $T_l=0$, $B=4\times10^{-4}$	$t<0.3s$ Refe. $J=2\times1.74\times10^{-4}$	$0.3s\le t<0.5s$ Refe. $J=1.74\times10^{-4}$	$0.5s\le t$ Refe. $J=2\times1.74\times10^{-4}$
case2	Refe. $B=4\times10^{-4}$, $J=1.74\times10^{-4}$	$t<0.3s$ Refe. $T_L=0$	$0.3s\le t<0.5s$ Refe. $T_L=2.4$	$0.5s\le t$ Refe. $T_L=0$
case3	Refe. $B=4\times10^{-4}$, $J=1.74\times10^{-4}$	$t<0.3s$ Refe. $T_L=0$	$0.3s\le t<0.5s$ Refe. $T_L=2.4sin(8\pi t)$	$0.5s\le t$ Refe. $T_L=0$

Note: "Refe." represents "Referenced".

TABLE 2. Parameters of the PMSM.

Parameters	Values/Units
Rated power	$0.75(Kw)$
Pole pairs	5
Rated speed	$3000(rpm)$
Moment coefficient	$0.14(N\cdot m/A)$
Line inductance	$0.3(mh)$
Line resistance	$0.08(\Omega)$
Rated torque	$2.4(N\cdot m)$
Rate current	17.5(A)

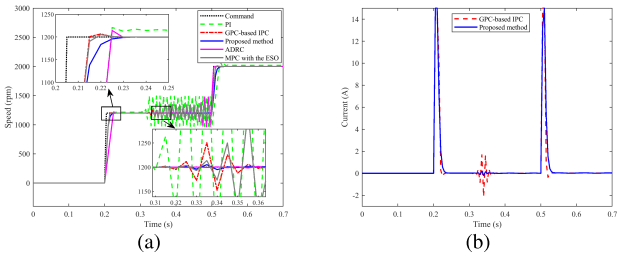

(a) (b)

FIGURE 4. Speed responses and torque currents at Case 1.

feedback speed and current at the same time. 5) The load torque is added by adopting a magnetic powder brake. Note that the initialization settings and parameter configurations are consistent with the simulation. Due to the limitation that the experimental platform cannot change the inertia, two experimental cases, i.e., the fixed load torque and the time-varying load torque in sinusoidal form, are tested to verify the control performance of the proposed method.

The speed responses of these five controllers are shown in Fig. 11(a). Before $t = 1s$, no load torque is applied to the PMSM. When $t = 0.5s$, the command is abruptly changed, all the PIC, the ADRC,the MPC with ESO method,

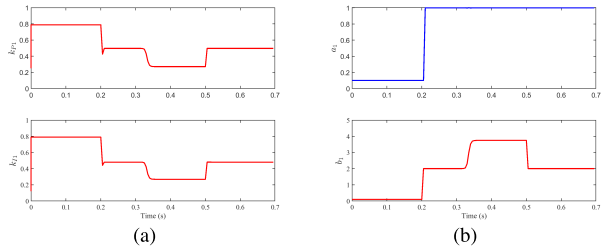

FIGURE 5. Control parameters and model parameters at Case 1.

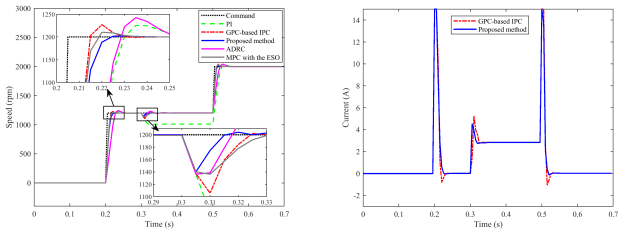

FIGURE 6. Speed responses and torque currents at Case 2.

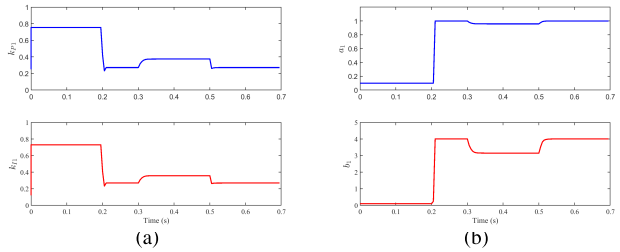

FIGURE 7. Control parameters and model parameters at Case 2.

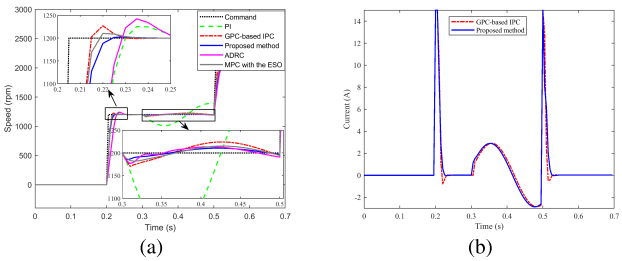

FIGURE 8. Speed responses and torque currents at Case 3.

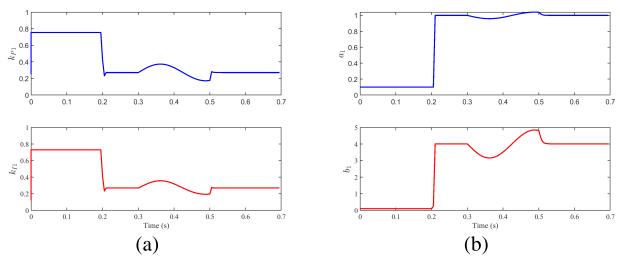

FIGURE 9. Control parameters and model parameters at Case 3.

and the GPC-based controller show obvious overshoot, and in contrast, the proposed method can significantly reduce the overshoot by smoothing the speed command. When $1 \leq t \leq 1.5s$, $T_l = 2.4N \cdot m$ is added to the PMSM, it is easy to see that the speed response of five controllers has declined to

TABLE 3. The quantitative comparison of the five controllers.

test	Mothods	$0.3s \leq t < 0.5s$		
		RMSE (rpm)	ST (s)	MOA (rpm)
Fig.4(a)	The fixed PI controller	0.2268	0.025	292
	The ADRC method in [5]	0.1535	None	277
	The MPC with the ESO in [8]	0.0998	0.065	145
	The GPC-based IPC	0.0118	0.060	50
	The proposed scheme	0.0014	0.045	5
Fig.6(a)	The fixed PI controller	0.1718	0.035	197
	The ADRC method in [5]	0.0182	0.035	62
	The MPC with the ESO in [8]	0.0147	0.030	64
	The IGPC-based IPC	0.0177	0.020	94
	The proposed scheme	0.0095	0.010	60
Fig.8(a)	The fixed PI controller	0.1278	None	187
	The ADRC method in [5]	0.0091	0.020	23
	The MPC with the ESO in [8]	0.0116	0.025	21
	The IGPC-based IPC	0.0154	0.025	30
	The proposed scheme	0.0069	0.015	16

TABLE 4. The quantitative comparison of the five controllers.

test	Mothods	$1s \leq t < 1.5s$		
		RMSE (rpm)	ST (s)	MOA (rpm)
Fig.11(a)	The fixed PI controller	0.1107	0.045	150
	The ADRC method in [7]	0.029	0.055	134
	The MPC with the ESO in	0.0284	0.050	161
	The GPC-based IPC	0.0732	0.035	251
	The proposed scheme	0.0210	0.015	92
Fig.13(a)	The fixed PI controller	0.0805	None	110
	The ADRC method in [7]	0.0085	0.035	22
	The MPC with the ESO in	0.0091	0.040	29
	The GPC-based IPC	0.0528	None	66
	The proposed scheme	0.0050	0.030	11

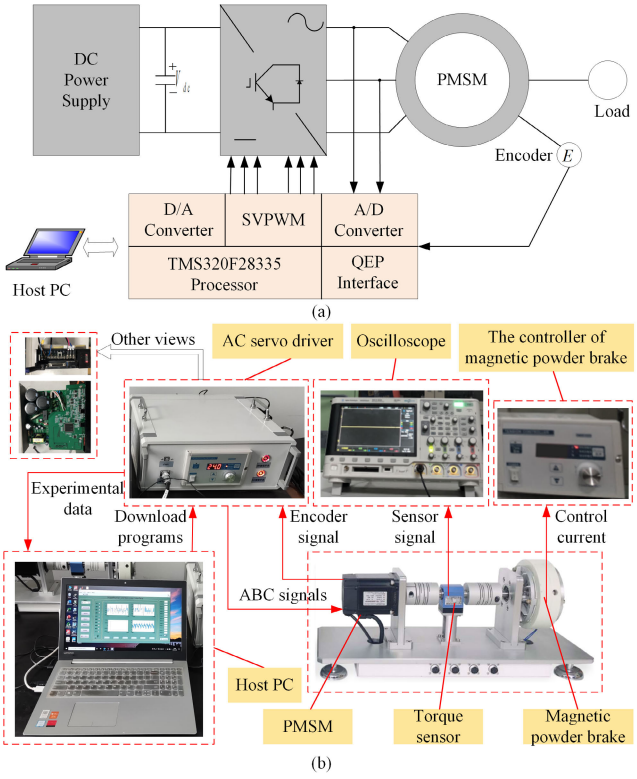

FIGURE 10. Overall experiment platform.

varying degrees, but it is apparent that the proposed method, the MPC with ESO in [8], and the ADRC in [5] are superior to the other two controllers in terms of decreased amplitude

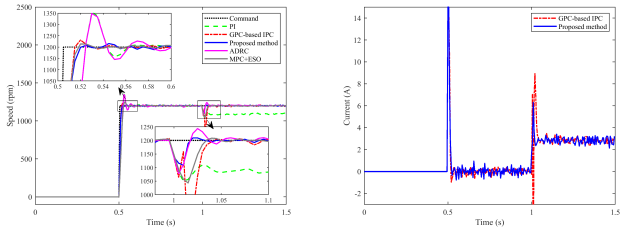

(a) (b)

FIGURE 11. Speed responses and torque currents with the fixed load torque.

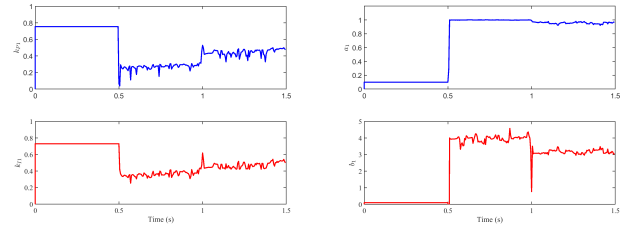

(a) (b)

FIGURE 12. Control parameters and model parameters with the fixed load torque.

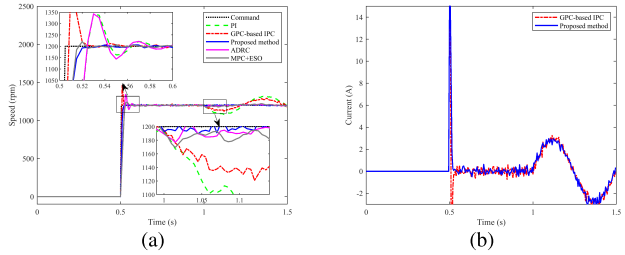

(a) (b)

FIGURE 13. Speed responses and torque currents with the sinusoidal load torque.

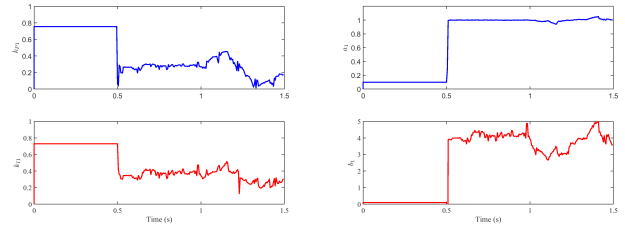

(a) (b)

FIGURE 14. Control parameters and model parameters with the sinusoidal load torque.

and convergence speed. Compared to the speed response in simulation, more notably, the GPC-based IPC suffers from larger velocity spikes and longer regulation time in the experimental results, which is due to the model mismatch of the identification convergence process that poses a serious challenge to the model-based adaptive controller. Fig. 11(b) shows the torque current, and the control parameters and model parameters of the proposed method are shown in Fig. 12.

Meanwhile, the speed response of the system with the time-varying load torque $T_l = 2.4sin(4\pi t)N \cdot m$ shown in Fig. 13(b) can also demonstrates the advantages of the proposed method, which almost avoids the adverse effects caused by model mismatch, and in comparison to the ADRC method and the MPC with ESO method, the oscillation amplitude of our method is smaller. In addition, Table 4 illustrates a quantitative comparison of these three controls involving RMSE, ST, and MOA. This comprehensively validates the advantages of the proposed method in terms of control performance, robustness, and immunity to interference.

VI. CONCLUSION

The PMSM servo system is now widely used in industrial applications, and the traditional controllers are no longer suitable for rapidly growing industrial requirement. To improve the tracking performance of the PMSM servo system, an adaptive controller structure based on the GPC law is proposed in this paper. It is worth mentioning that the GPC law is used to provide control parameters for two controllers simultaneously, which greatly improve the control performance, especially during the model mismatch. Extensive theoretical analysis as well as comprehensive simulation and experimental results indicate that the proposed method is significantly competitive compared to existing methods, including the PIC, the ADRC, the MPC with ESO, and the GPC-based IPC. In future research, we will focus on the application of proposed method to the servo drive of industrial robots.

REFERENCES

[1] E. Lu, W. Li, S. Jiang, and Y. Liu, "Anti-disturbance speed control of permanent magnet synchronous motor based on fractional order sliding mode load observer," *IEEE Access*, early access, Oct. 13, 2022, doi: 10.1109/ACCESS.2022.3214205.

[2] H. Chang, S. Lu, G. Huang, S. Zheng, and B. Song, "An extended active resonance suppression scheme based on a dual-layer network for high-performance double-inertia drive system," *IEEE Trans. Power Electron.*, vol. 38, no. 11, pp. 13717–13729, Nov. 2023.

[3] T. T. Nguyen, T. H. Nguyen, and J. W. Jeon, "Explicit model predictive speed control for permanent magnet synchronous motor with torque ripple minimization," *IEEE Access*, vol. 11, pp. 134199–134210, 2023.

[4] J.-K. Seok, K.-T. Kim, and D.-C. Lee, "Automatic mode switching of P/PI speed control for industry servo drives using online spectrum analysis of torque command," *IEEE Trans. Ind. Electron.*, vol. 54, no. 5, pp. 2642–2647, Oct. 2007.

[5] Y. Zuo, J. Mei, C. Jiang, X. Yuan, S. Xie, and C. H. T. Lee, "Linear active disturbance rejection controllers for PMSM speed regulation system considering the speed filter," *IEEE Trans. Power Electron.*, vol. 36, no. 12, pp. 14579–14592, Dec. 2021.

[6] N. Guler, S. Bayhan, U. Fesli, A. Blinov, and D. Vinnikov, "Super twisting sliding mode control strategy for input series output parallel converters," *IEEE Access*, vol. 11, pp. 107394–107403, 2023.

[7] X. Wang, B. Wang, X. Chen, and J. Yu, "Discrete-time position tracking control for multimotor driving systems via multipower terminal sliding-mode technique," *IEEE/ASME Trans. Mechatronics*, early access, Jul. 28, 2024, doi: 10.1109/TMECH.2023.3295510.

[8] L. Sun, X. Li, L. Chen, H. Shi, and Z. Jiang, "Dual-motor coordination for high-quality servo with transmission backlash," *IEEE Trans. Ind. Electron.*, vol. 70, no. 2, pp. 1182–1196, Feb. 2023.

[9] L. Sun, X. Li, and L. Chen, "Motor speed control with convex optimization-based position estimation in the current loop," *IEEE Trans. Power Electron.*, vol. 36, no. 9, pp. 10906–10919, Sep. 2021.

[10] J. Cai, F. Qian, R. Yu, and L. Shen, "Adaptive backstepping control for a class of non-triangular structure nonlinear systems," *IEEE Access*, vol. 8, pp. 76093–76099, 2020.

[11] B. Wang, M. Iwasaki, and J. Yu, "Command filtered adaptive backstepping control for dual-motor servo systems with torque disturbance and uncertainties," *IEEE Trans. Ind. Electron.*, vol. 69, no. 2, pp. 1773–1781, Feb. 2022.
[12] A. Lokriti, I. Salhi, S. Doubabi, and Y. Zidani, "Induction motor speed drive improvement using fuzzy IP-self-tuning controller. A real time implementation," *ISA Trans.*, vol. 52, no. 3, pp. 406–417, May 2013.
[13] Y. Bekakra, Y. Labbi, D. Ben Attous, and O. P. Malik, "Rooted tree optimization algorithm to improve DTC response of DFIM," *J. Electr. Eng. Technol.*, vol. 16, no. 5, pp. 2463–2483, Sep. 2021.
[14] R. K. Mahto and A. Mishra, "Self-tuning vector controlled PMSM drive using particle swarm optimization," in *Proc. IEEE 1st Int. Conf. Smart Technol. Power, Energy Control (STPEC)*, Nagpur, India, Sep. 2020, pp. 1–5.
[15] Y. Wang, Q. Jin, and R. Zhang, "Improved fuzzy PID controller design using predictive functional control structure," *ISA Trans.*, vol. 71, pp. 354–363, Nov. 2017.
[16] O. Rodríguez-Abreo, J. Rodríguez-Reséndiz, C. Fuentes-Silva, R. Hernández-Alvarado, and M. D. C. P. T. Falcón, "Self-tuning neural network PID with dynamic response control," *IEEE Access*, vol. 9, pp. 65206–65215, 2021.
[17] H. Xu, S. Li, L. Zhang, and H. Liu, "Two-degree-of-freedom PID boiler steam temperature control method based on the internal model principle," in *Proc. 37th Chin. Control Conf. (CCC)*, Wuhan, China, Jul. 2018, pp. 3420–3424.
[18] Y. Kansha, L. Jia, and M.-S. Chiu, "Self-tuning PID controllers based on the Lyapunov approach," *Chem. Eng. Sci.*, vol. 63, no. 10, pp. 2732–2740, May 2008.
[19] T. Sato, "Design of a GPC-based PID controller for controlling a weigh feeder," *Control Eng. Pract.*, vol. 18, no. 2, pp. 105–113, Feb. 2010.
[20] S. Lu, F. Zhou, Y. Ma, and X. Tang, "Predictive IP controller for robust position control of linear servo system," *ISA Trans.*, vol. 63, pp. 211–217, Jul. 2016.
[21] W. Qiao, X. Tang, S. Zheng, Y. Xie, and B. Song, "Adaptive two-degree-of-freedom PI for speed control of permanent magnet synchronous motor based on fractional order GPC," *ISA Trans.*, vol. 64, pp. 303–313, Sep. 2016.
[22] H. Chang, S. Lu, S. Zheng, B. Song, and J. Yang, "Integration of predictive control and interconnected structure for autotuning velocity controller," *IEEE/ASME Trans. Mechatronics*, vol. 28, no. 6, pp. 3250–3262, Dec. 2023.
[23] X. Liu, C. Zhang, K. Li, and Q. Zhang, "Robust current control-based generalized predictive control with sliding mode disturbance compensation for PMSM drives," *ISA Trans.*, vol. 71, pp. 542–552, Nov. 2017.
[24] I. Koryakovskiy, M. Kudruss, H. Vallery, R. Babuška, and W. Caarls, "Model-plant mismatch compensation using reinforcement learning," *IEEE Robot. Autom. Lett.*, vol. 3, no. 3, pp. 2471–2477, Jul. 2018.
[25] J. Lai, X. Yin, Z. Zhang, Z. Wang, Y. Chen, and X. Yin, "System modeling and cascaded passivity based control for distribution transformer integrated with static synchronous compensator," *Int. J. Electr. Power Energy Syst.*, vol. 113, pp. 1035–1046, Dec. 2019.
[26] S. Lu, S. Zhang, H. Chang, S. Zheng, and B. Song, "Speed-command-independent parameters self-tuning and mismatch compensation for servo speed control," *Control Eng. Pract.*, vol. 137, Aug. 2023, Art. no. 105550.
[27] J. Lara, J. Xu, and A. Chandra, "Effects of rotor position error in the performance of field-oriented-controlled PMSM drives for electric vehicle traction applications," *IEEE Trans. Ind. Electron.*, vol. 63, no. 8, pp. 4738–4751, Aug. 2016.
[28] F. Morel, X. Lin-Shi, J.-M. Retif, B. Allard, and C. Buttay, "A comparative study of predictive current control schemes for a permanent-magnet synchronous machine drive," *IEEE Trans. Ind. Electron.*, vol. 56, no. 7, pp. 2715–2728, Jul. 2009.
[29] S. Bolognani, S. Bolognani, L. Peretti, and M. Zigliotto, "Design and implementation of model predictive control for electrical motor drives," *IEEE Trans. Ind. Electron.*, vol. 56, no. 6, pp. 1925–1936, Jun. 2009.
[30] H. Liu and S. Li, "Speed control for PMSM servo system using predictive functional control and extended state observer," *IEEE Trans. Ind. Electron.*, vol. 59, no. 2, pp. 1171–1183, Feb. 2012.

FENG DAN received the B.S. and Ph.D. degrees in computer science from Wuhan University, Wuhan, China, in 2003 and 2013, respectively.

He is currently a Lecturer with the College of Information Science and Engineering, Wuhan University of Science and Technology, Wuhan. His research interests include intelligent control, mobile communications, software engineering, and the Internet of Things.

HUILAN HE received the B.S. degree in traffic engineering from Wuyi University, in 2018. She is currently pursuing the M.S. degree in electronic information with Wuhan University of Science and Technology, Wuhan, China.

Her research interest includes automated control.

SHAOWU LU received the Ph.D. degree in mechanical engineering from Huazhong University of Science and Technology, China, in 2013.

He is currently a Professor with Wuhan University of Science and Technology, Wuhan, China. His current research interests include system identification, servo control, and intelligent control.

YAJIE MA received the B.S. degree in automation from Wuhan University of Science and Technology, Wuhan, China, in 1996, and the M.S. degree in circuit and system and the Ph.D. degree in communication and information engineering from Huazhong University of Science and Technology, Wuhan, in 2000 and 2005, respectively.

From 2006 to 2009, she was a Research Associate with the Department of Computing, Imperial College London, London, U.K. Since 2013, she has been a Professor with the College of Information Science and Engineering, Wuhan University of Science and Technology. She has been intensively working on protocol design, topology optimization, and data analysis in wireless sensor networks. Her research interests include underwater acoustic sensor networks, data quality management, and the Internet of Vehicles.